Sparse incomplete LU-decomposition for Wave Farm Designs under Realistic Conditions

Dídac Rodríguez Arbonès[1,4], Nataliia Y. Sergiienko[2], Boyin Ding[2], Oswin Krause[1], Christian Igel[1], and Markus Wagner[3]

[1] Department of Computer Science, University of Copenhagen, Denmark
[2] School of Mechanical Engineering, University of Adelaide, Australia
[3] School of Computer Science, University of Adelaide, Australia
[4] NETS A/S, Denmark

Abstract. Wave energy is a widely available but still largely unexploited energy source, which has not yet reached full commercial development. A common design for a wave energy converter is called a point absorber (or buoy), which either floats on the surface or just below the surface of the water. Since a single buoy can only capture a limited amount of energy, large-scale wave energy production requires the deployment of buoys in large numbers called arrays. However, the efficiency of these arrays is affected by highly complex constructive and destructive intra-buoy interactions.
We tackle the multi-objective variant of the buoy placement problem: we are taking into account the highly complex interactions of the buoys, while optimising critical design aspects: the energy yield, the necessary area, and the cable length needed to connect all buoys. We do all this while considering realistic wave conditions for the first time, i.e., a real wave spectrum and waves from multiple directions. To make the problem computationally feasible, we use sparse incomplete *LU* decomposition for solving systems of equations, and caching of integral computations. For the optimisation, we employ modern multi-objective solvers that are customised to the buoy placement problems. We analyse the wave field of final solutions to confirm the quality of the achieved layouts.

1 Introduction

With ever-increasing global energy demand and finite reserves of fossil fuels, renewable forms of energy are becoming increasingly important to consider [14]. Wave energy is a widely available but unexploited source of renewable energy with the potential to make a considerable contribution to future energy production [12]. A multitude of techniques for extracting wave energy are currently being explored [12, 13].

A wave energy converter (WEC) is a device that captures and converts wave energy to electricity. One common WEC design is the point absorber or buoy, which typically floats on the surface or just below the surface of the water, and captures energy from the movement of the waves [12].

In our research, we consider three-tether WECs (Figure 1) inspired by the next generation of CETO systems developed by the Australian wave energy company called Carnegie Clean Energy. These buoys operate under water surface (fully submerged) and tethered to the seabed in an offshore location.

Fig. 1: Schematic representation of a three-tether WEC [24].

One of the central goals in designing and operating a wave energy device is to maximise its overall energy absorption. As a result, the optimisation of various aspects of wave energy converters is an important and active area of research. Three key aspects that are often optimised are geometry, control, and positioning of the WECs within the wave energy farm (or array). Geometric optimisation seeks to improve the shape and/or dimensions of a wave energy converter (or some part of it) with the objective of maximising energy capture [15, 17]. On the other hand, the optimisation of control is concerned with finding good strategies for actively controlling a WEC [19]. A suitable control strategy is needed for achieving high WEC performance in real seas and oceans, due to the presence of irregular waves [6]. In this article we focus on the third aspect, namely the positioning of multiple wave energy converters while considering constraints, additional objectives, and realistic wave conditions.

To evaluate the performance of our arrays, we use a frequency domain model for arrays of fully submerged three-tether WECs [21]. This model enables us to investigate design parameters, such as number of devices and array layout. In addition to the objective of producing energy, we consider two more objectives: the area needed to place all buoys, and the cable length needed to connect all buoys. This results in an optimisation problem: what are the best trade-offs of the the area needed, the buoys' locations, and the cable length needed? To the best of our knowledge, this study is the first to investigate this question to reduce costs and to increase efficiency, *while considering realistic wave conditions.* A first related study is that by Wu et al. [24] where a single objective (power output) was considered and only a single wave frequency and single direction to keep the computational cost at bay. Arbonès et al. [1] investigated multiple objectives by considering parallel architectures and varying numbers of wave frequencies, while again being limited to a single wave direction.

We take this as a starting point for our four contributions here: (i) we use a realistic wave scenario with multiple directions, (ii) we speedup the calculations, (iii) we employ a different constraint handling approach to allow the use of other algorithms, and (iv) we provide insights by characterising the wave field.

We proceed as follows. In Section 2, we describe the WEC power generation model used in our study and introduce the multi-objective buoy placement problem. We describe the different objectives that are subject to our investigations, and the constraints used and how we implemented them. We note the problem complexity, which is the factor preventing study of large farms. Then, we present in Section 3 our methods to reduce running times and the constraint handling used. We describe and present our experiments in Section 4, provide a discussion of the results in Section 5, and conclude with a summary in Section 6.
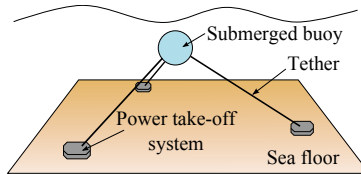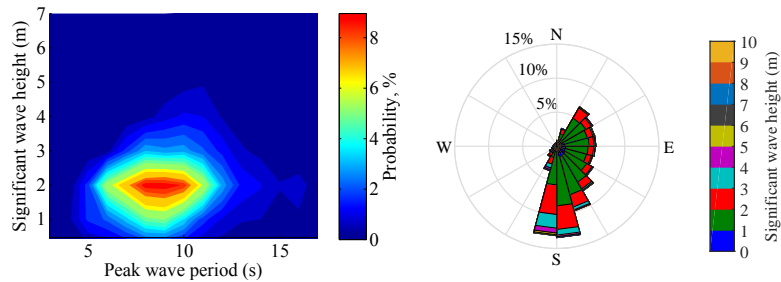
Fig. 2: Australia/New South Wales (NSW) test site near Sydney: wave data statistics (left) and the directional wave rose [2] (right).

2 Preliminaries

The total performance of a wave energy farm is not only dependent on the number of WEC units in the array, but also on their mutual arrangement and separating distances. The total capital expenditure per single unit decreases significantly with increase in the farm scale [18]. When operating in a group, WECs interact with each other modifying the incident wave front which can lead to the significant reduction in generated power [3]. Moreover, the interference between converters can be destructive as well as constructive which purely depends on their hydrodynamic parameters and coupling. Thus, the array layout is of great importance for the efficient operation of the whole farm, as well as the wave conditions (dominant wave periods and wave directions).

The WEC chosen for this study is a fully submerged spherical buoy connected to three tethers (taut moored) that are equally distributed around the buoy hull (Figure 1). Each tether is attached to the individual power generator at the sea floor, which allows to extract energy from surge and heave motions simultaneously [20]. The geometric parameters of the buoys are as follows: they have a 5m radius, are submerged at 6m below the water surface, have a weight of 376 tons, and the tether inclination angle from the vertical is 55 degrees. A particular site on the east coast of Australia has been selected as one of the potential locations for the farm installation (see Figure 2 for sea site statistics).

2.1 Objectives

We consider a multi-objective optimisation scenario, using various evolutionary algorithms, where multiple goals are leveraged to obtain a set of solutions.

Power Output. The frequency domain model of this kind of WEC arrays has been derived by Sergiienko et al. [21], and used by in related work [1, 24]. In the model, the hydrodynamic interaction of submerged spheres is taken from [23] and the machinery force of each power take-off unit is modelled as a linear spring-damper system. The output from the model is a power absorbed by the array of WECs $P(\mathbf{x}, \mathbf{y}, \omega, \beta)$ that is a function of their spatial position (coordinates) $(\mathbf{x}, \mathbf{y})$, wave frequency ω, and wave angle β.

As a result, the optimisation problem that corresponds to the power production of the array is expressed:

$$\max_{(\mathbf{x},\mathbf{y})} \int\limits_{\beta} f_{\beta} \cdot \left(\int\limits_{\omega} f_{\omega} \cdot P(\mathbf{x}, \mathbf{y}, \omega, \beta) \, \mathrm{d}\omega \right) \mathrm{d}\beta, \tag{1}$$

There is no closed form solution for this equation. The result is computed by a discrete set of wave frequencies and angles sampled from the distribution.

Additional objectives. As the second objective after the wave farm's power output, we use the Euclidean minimum spanning tree (MST) to calculate the minimum length of cable or pipe required to connect all buoys.

Thirdly, the cost of the convex hull is defined as the area contained by the set of buoys that form the convex hull. This corresponds to the minimum land area that is required for a wave farm layout. While we omit it here, a safety distance at the perimeter of the wave farm should be included for production purposes.

Constraints. The problem uses two types of constraints. Box constraints restrict the available sea surface, and prevent the use of unrealistic amounts of space. The second constraint ensures that no two buoys are placed closer than 50m. This prevents damage and allows for installation and maintenance ships (such as the Atlantic Hawk vessel) to navigate between the buoys safely.

2.2   Problem complexity

The main computational burden is coming from the evaluation of the power output, which involves (i) the approximation of singular numerical integrals involved in the hydrodynamic model [23], and (ii) solution of the linear system of $3 \times N$ motion equations of the form $Ax = b$, where N corresponds to the number of buoys in the array. As a result, the complexity of a function evaluation depends on a number of factors, including, but not limited to, the number of buoys, wave directions and number of frequencies considered. To obtain a reliable power prediction, we sample a set of wave frequencies and angles. The accuracy of the result depends on quantity and probability of parameters chosen. Therefore there is an accuracy/time trade-off. The problem quickly becomes untractable for farm sizes of practical interest. In this article, we prioritize reducing the runtime of the power output computation to obtain the largest benefits.

Furthermore, the interbuoy-distance constraint is non-convex, which prevents the use of some algorithms that cannot handle this type of constraints. Relaxation of this constraint is not considered, as it would discard potentially good solutions.

3   Computational speed-ups and constraint handling

Numerical integration. The integrals in the hydrodynamic model span over an infinite interval and contain a singularity at some point K. To obtain an approximation, we use an implementation of Cauchy principal value for the interval $(0, 1.5K)$, and an algorithm based on a 21-point Gauss-Kronrod rule (provided by the GNU Scientific Library [5]) for the remaining infinite interval.

(a) Random initialisation of 4 Buoys

(b) Random initialisation of 9 Buoys

(c) Random initialisation of 36 Buoys
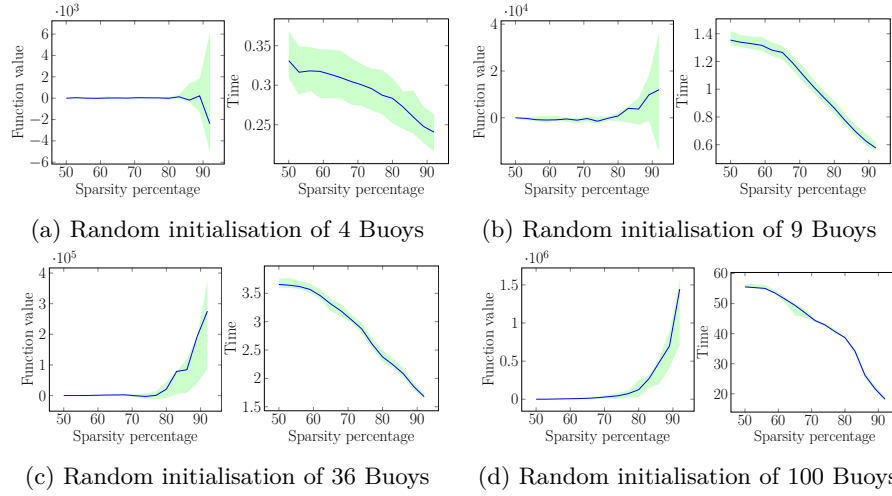
(d) Random initialisation of 100 Buoys

Fig. 3: Relative power output (left) and time per iteration (right), against sparsity percentage; medians of 100 runs (blue), 5%/95% percentiles (green).

Caching. During evaluation of the power output function, the integral is evaluated several times with different parameters, pertaining to the positioning of the buoys. These integrals appear often with the same parameters, and thus, do not have to be recomputed. We cache the results, which allows for a more efficient use of computational resources and avoids unnecessary calculations.

Linear algebra. The linear systems of the form $Ax = b$ become the bottleneck after the approximation of the integrals. The typical choice for solving this type of system of equation is the LU-factorization with partial pivoting. However, for our application this approach is too slow as we need to solve several thousand systems of equations throughout the optimisation process. Instead, we make use of the fact that this system has many variables with values very close to zero and thus their contribution to the final solution is negligible. One approach is to compute a sparse incomplete LU-decomposition as a pre-conditioner for an iterative algorithm. This procedure adds the cost of computing the approximate decomposition in trade for fast solving of the system of equations. This approach works best when the system has to be solved with several right hand sides as in this case, where the cost of computing the LU-decomposition amortises.

In our case, we can not reuse the LU-decomposition. Instead we use the fact that for a low percentage of zero-entries the incomplete LU-decomposition gives a good approximation to the original system. Thus we can approximate the original system by a sparse variation where we discard the smallest percentile of values and solve it approximately using the incomplete LU-decomposition. This saves time approximately linear in the percentage of discarded values.

We have to evaluate experimentally at which percentage of discarded values we can still obtain a reasonable accuracy. For this, we generate 100 random feasible buoy layouts. While keeping the layouts fixed, we discard values and compare the computed power output to the dense solution.
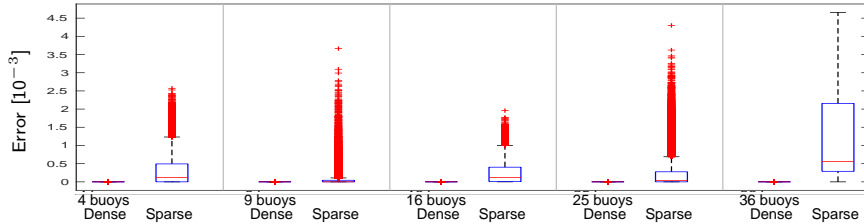
Fig. 4: Relative residual error of 100 different random feasible layouts using dense and sparse solver. For the sparse, 70% of the smallest values were discarded.

Figure 3 shows the obtained solutions with respect to matrix sparsity, where the power output of each layout has been subtracted for comparison. We can see that run-time decreases linearly with the increasing number of discarded values. The accuracy of the solution remains stable until 75% sparsity, where it starts to degrade. The accuracy loss of the 70% sparse solution with respect to the dense implementation is shown in Figure 4. To obtain the error of the linear system $Ax = b$, we use the formula $\|As - b\|/\|b\|$, where s is the solution obtained.

Constraint handling. The box constraint to allow buoy placements only in the designated area is enforced by a sinusoidal function of the form [7]: $x = a + (b - a) * (1 + \cos(\pi * x/(b - a) - \pi))/2$. The range of this function is (a, b), and provides a smooth transition near the boundaries which is beneficial for the algorithms. By setting $a, b \in \mathbb{R}$ to the box limits, we guarantee that any solution obtained will lay within the feasible range.

We implemented the inter-buoy constraint with a penalty function proportional to the square of the violation distance. The function takes the set of all buoys $(\boldsymbol{b}_1 \ldots \boldsymbol{b}_n)$, and a minimum distance parameter M: $\mathrm{v}(\boldsymbol{b}_1 \ldots \boldsymbol{b}_n) = \sum_{i=1}^{n} \sum_{j \neq i}^{n} \max(M^2 - \|\boldsymbol{b}_i - \boldsymbol{b}_j\|^2, 0)$. The objectives $\boldsymbol{F}$ of a given layout are then scaled according to a penalty regularisation parameter K: $\boldsymbol{F'} = \boldsymbol{F}(1 + K\,\mathrm{v})$.

4   Experimental Study

Experimental Setup. To obtain a realistic output estimate and to generate solutions robust to the changing nature of the sea we choose to use 25 linearly-spaced frequencies and 7 wave directions sampled from Figure 2. Note that a direction of 0° indicates waves coming from the south.

We run experiments for farms of 4, 9, 16, 25 and 36 buoys. We set the boundaries of the farm depending on the amount of buoys to be placed, using 20.000 m^2 per buoy. This results in squares of sides 283m, 424m, 566m, 707m, and 849m. We limit most of our report here to 4, 9, and 36 buoys.

We use Unbounded-Population-MO-CMA-ES (UP-MO-CMA-ES) [11], Steady-State-MO-CMA-ES (SS-MO-CMA-ES) [9], SMS-EMOA [4]. Furthermore, for comparison purposes, we use the variant of SMS-EMOA with custom operators presented in [1] (SMS-EMOA*). These operators are specific to our kind of placement problem and have been used in wind farm turbine placement as well as WEC placement optimisation [1, 22]. In particular, Move-mentMutation moves single WECs along corridors for local search purposes, and BlockSwapCrossover recombines sub-layouts from complete layouts in
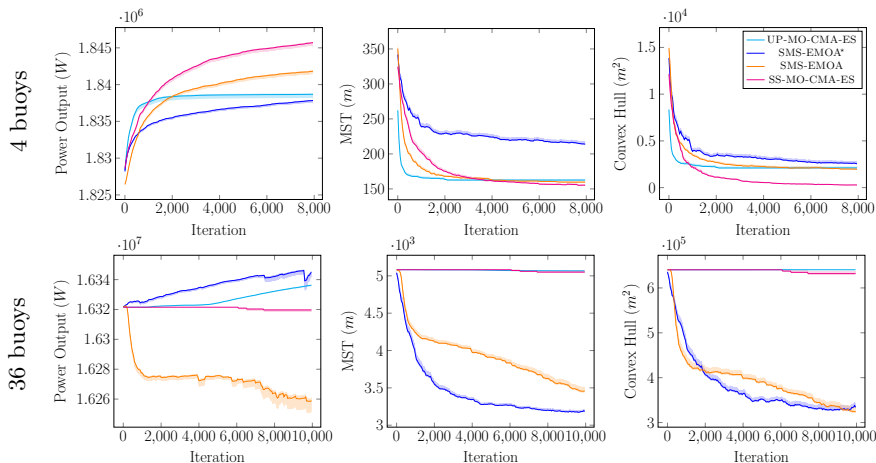
Fig. 5: Evolution of the three objectives for all algorithms. Shown are the means of 100 runs with 75% confidence intervals.

order to potentially recombine good sub-layouts into higher-performing ones. We run each combination of algorithm and amount of buoys 100 times.

We initialise with a population size of $\mu = 50$, and run the experiments for 8000 iterations (for 25 and 36 buoys the budget is 10000). For SS-MO-CMA-ES and UP-MO-CMA-ES we set $\sigma = 50$. We initialise the algorithms with $\mu = 50$ grids of different sizes, i.e., from the smallest grid (inter-buoy distance 50 meters) to the largest grid where the outermost buoys are at the boundary.

We use $K = 100$ in the regularisation of infeasible layouts, as we found this to be a good trade-off between preventing the algorithms from using infeasible solutions, and allowing exploration of regions close to the boundaries.

We focus on the power output because it is the objective of highest practical importance. The convex hull and minimum spanning tree attempt to decrease the cost and resource utilization of the final solution, while the power output is the target driving the funding and development of the farm infrastructure.

Experimental Results. We present the results of our experiments for the different multi-objective algorithms used. Our inter-buoy penalty does not guarantee that infeasible solutions will not be produced, therefore we ignore them here.

As the power objective is most important, we first present the evolution of the points with the highest power output. For all farm sizes considered, we show the means over the points with highest power output of all fronts and their 75% confidence intervals for each iteration. Additionally, Figure 5 shows the values of minimum spanning tree (MST) and convex hull (CH) of those points.

To compare the performance of the multi-objective algorithms we use the so-called hypervolume, which is the volume of the space dominated by the found solutions and a chosen reference point as in [4]. We show the evolution of the volume over the course of optimisation in Figure 6 for all algorithms.

In Figure 7, we show the set of non-dominated feasible solutions found by any algorithm after the last iteration. The objective value achieved by the layouts with highest power outputs are given in Table 1. As we can see, the power output

Buoys	Highest power initial solution			Highest overall power solution		
	Power (MW)	MST (m)	CH (m^2)	Power (MW)	MST (m)	CH (m^2)
4	1.8258	396	17635	1.8497	152.29	10.8
9	4.1042	1008	63635	4.1590	493	10465
16	7.2873	1734	124906	7.3254	1263	98797
25	11.3506	2520	183542	11.4145	1823	156958
36	16.3215	5082	640442	16.3757	3080	323946

Table 1: Objectives attained by initial and optimised individuals.

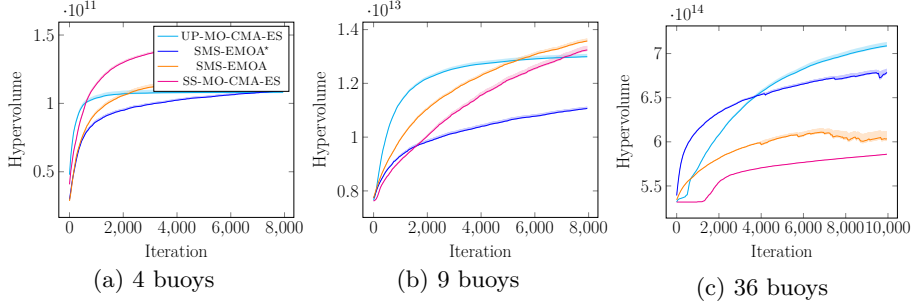(a) 4 buoys   (b) 9 buoys   (c) 36 buoys

Fig. 6: Hypervolumes: means of 100 runs with 75% confidence intervals. The reference point is based on the worst values obtained for each objective.

of the best solutions always increased slightly over the initial best layouts, while the MST length and the area needed both decreased significantly. This means that the newly found layouts not only produce more energy, but also require shorter pipes and a smaller area.

5   Discussion

Optimisation interpretation. The modified SMS-EMOA worked better for the best individuals except in 4 dimensions. In terms of hypervolume, the UP-MO-CMA consistently outperformed the other variants for larger layouts. We obtained a roughly 1% improvement on average over the best initial grid.

The SS-MO-CMA-ES consistently performs well on the 4-buoy layout, however it becomes worse on the larger layouts and fails for layouts with more than 9 buoys. The UP-MO-CMA-ES performs better in comparison. We argue that the reason for this is the complex function landscape with constraints in conjunction with the different measures of progress. The UP-MO-CMA-ES only requires a point to be non-dominated to make progress. Thus it have more chances to adapt to the function landscape. The SS-MO-CMA-ES in comparison must create points which non-dominated but also an improvement in covered volume. Thus the SS-MO-CMA-ES will quickly adapt to evaluate solutions close to existing solutions and thus might easily get stuck in local optima.

The SMS-EMOA has good performance when used in farm sizes of 4 buoys, but lags behind for larger farms. In contrast, SMS-EMOA* consistently outperforms all other algorithms and produces the best solutions. This shows that the operators developed for wind turbine placement generalise to the similar task of WEC positioning. However, in terms of of hypervolume covered, it lags behind the UP-MO-CMA-ES.
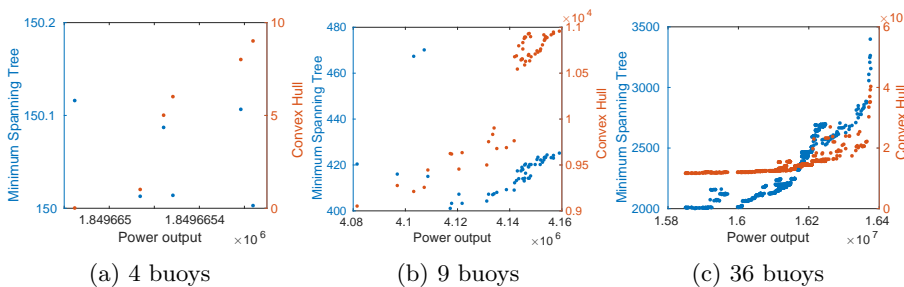
(a) 4 buoys (b) 9 buoys (c) 36 buoys

Fig. 7: Aggregated fronts of all algorithms' non-dominated solutions. The three dimensional objective space is plotted twice into the two-dimensional space.

One might wonder whether our best performing layouts (in terms of power output) are optimal. While we have no means of proving optimality, we do know that the UP-MO-CMA-ES used in the experiment uses 20% of the given budget on the corner points. This means it spends a considerable amount of effort on exploring extreme trade-offs, among which are the layouts with highest power output. Therefore, the results of UP-MO-CMA-ES given here provide a good intuition of how UP-MO-CMA-ES's single-objective cousin CMA-ES [8] would perform, albeit with a smaller budget.

Hydrodynamic interpretation. In order to analyse the optimisation results, it is necessary to understand how a particular array layout modifies the wave field and how much power propagates downstream as waves travel through the farm. Firstly, we explore the behaviour of the wave farm for the dominant wave period of 9 s ($\omega = 0.7$ rad/s) and the wave angle of 0°. For the following interpretation we use WAMIT, which a state-of-the-art tool used by the industry and research community for analysing wave interactions.

When a wave hits the buoy, a part of the wave front passes through the object creating a wake field behind, a part of the wave is diffracted back and the rest is absorbed by the converter. Other wave types are the radiated waves that spread uniformly in all directions from the oscillating structure (wave source). Depending on the phase information, these three types of waves can be superimposed on each other creating a more energetic wave field, or in other case they can eliminate each other leading to the smaller or zero wave amplitude. Thus, for the wave farm design it is important to place buoys in such locations when waves create a *constructive interaction* resulting in more wave power.

In Figure 8 (left), we show the wave energy transport per unit frontage of the incident and radiated wave for the 4-unit array. It can be seen that the initial square layout has two converters located in a wake of the first row which decreases their power output. The incident wave energy transport for this wave period is around 35 kW/m, while only 25 kW/m are propagated to the back row. As has been stated in [3], the park effect in the wave farm is the most significant for the front buoys as they benefit from radiated waves of a row behind. Interestingly, WECs in the optimised layout are lined up perpendicular to the wave front. An inter-buoy distance is about 51 m which is equal to 0.43λ, if we consider only one dominant frequency of the spectrum (here λ is a wavelength).
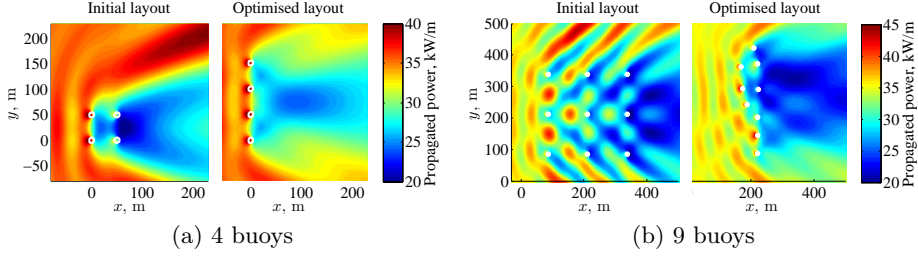
(a) 4 buoys   (b) 9 buoys

Fig. 8: The wave field around the 4 and 9-unit arrays of WECs with the initial (left) and optimised (right) layouts. White circles show the location of submerged spherical buoys. The wave propagates from left.

Comparing this result with existing literature, this particular scenario buoys should be separated by $0.85\lambda = 100$ m [10, 16] in order to achieve the maximum constructive interaction in the array leading to a quality factor of 1.5. However, the other optimisation objectives came into place limiting the inter-buoy distance.

Similar behaviour of the optimisation algorithm is observed for the case of 9 buoys (see Figure 8, right) resulting in the decreased number of rows as compared to the initial layout. From the hydrodynamic point of view, it would be even better to have only one row perpendicular to the wave front. However, single-line initialisation is not robust when a spectrum of wave directions is considered, and they would also require larger-than-allowed maximal dimensions.

With increasing number of units in the array, a more complex interaction between buoys takes place leading to the non-trivial optimisation results. In comparison to the 4-buoys array, more interesting effects can be observed looking at the wave field created by the 9-buoy array with the initial layout (see Figure 8 left). It becomes obvious that initially all converters have been placed to the areas, where radiated waves from adjacent buoys create disadvantageous conditions for power generation. In contrast, the coordinates of all converters in the optimised layout (see Figure 8 right) coincide with locations where more energy can be captured (similar to the local maxima on the surface plot), especially it is observed for the buoys placed in front.

Going deeper in the analysis, power outputs from all WECs within the 9-unit array are shown in Figure 9 for the initial and optimised layouts. As expected, for arrays with a regular grid (initial case), the amount of generated power from each row is reduced by about 10% as compared to the row ahead. In the final layout almost all WECs have power output higher than 450 kW, which proves the effectiveness of the optimisation algorithms.
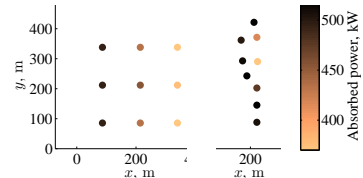

Fig. 9: Levels of absorbed power by the 9-unit arrays for the initial (left) and optimised (right) layouts. WECs sizes are not to scale.

6 Conclusions

Wave energy is widely available around the globe, however, it is a largely unexploited source of renewable energy. Over the last years, the interest in it has

increased tremendously, with dozens of wave energy projects being at various stages of development right now. In our studies we focused on point absorbers (also known as buoys). As the energy capture of a single buoy is limited, the deployment of large numbers of them is necessary to satisfy energy demands. In such scenarios, it is important to consider realistic intra-buoy interactions in order to optimise the operations of a wave energy farm.

In this article, we investigated the placement optimisation with respect to three competing objectives. To speed up the simulations of the intra-buoy interactions, we considered the use of sparse incomplete decompositions to solve linear systems. We tested different evolutionary optimisation algorithms, including custom variation operators developed for wind turbine placement. All simulations were done assuming realistic scenarios with waves coming from various directions with different probabilities and different wave spectra.

The volume covered by the solutions of the different algorithms showcases the complexity of the wave energy model for larger farm sizes. The highest power obtained from the experiments achieved a 1% increase in power on average over the best grid-based initial layout, translating to approximately 54 KW for a farm of 36 buoys. The extra annual energy production from the optimisation equates to the consumption of dozens of average households. In addition, the optimised layouts require significantly shorter cables (or pipes) for the interconnection, and a significantly smaller area for the installation.

In summary, our results show that the fast and effective multi-objective placement optimisation of wave energy farms under realistic conditions is possible and yields significant benefit. Furthermore, our results are consistent with previous results obtaining optimal separation between buoys.

Bibliography

[1] D. R. Arbonès, B. Ding, N. Y. Sergiienko, and M. Wagner. Fast and effective multi-objective optimisation of submerged wave energy converters. *Parallel Problem Solving from Nature*, pages 675–685, 2016.

[2] Australian Wave Energy Atlas, 2016. URL `http://awavea.csiro.au/`. Accessed 07 June 2016.

[3] A. Babarit. On the park effect in arrays of oscillating wave energy converters. *Renewable Energy*, 58:68 – 78, 2013.

[4] N. Beume, B. Naujoks, and M. Emmerich. SMS-EMOA: Multiobjective selection based on dominated hypervolume. *European Journal of Operational Research*, 181(3):1653–1669, 2007.

[5] GNU Scientific Library. *version 1.16*. 2013. URL `http://www.gnu.org/software/gsl/`. [Online; accessed 2-April-2017].

[6] J. Hals, J. Falnes, and T. Moan. A comparison of selected strategies for adaptive control of wave energy converters. *Journal of Offshore Mechanics and Arctic Engineering*, 133(3):031101, 2011.

[7] N. Hansen. CMA-ES Source Code: Practical Hints. `https://www.lri.fr/~hansen/cmaes_inmatlab.html`, 2014. [Online; accessed 2-April-2017].

[8] N. Hansen and A. Ostermeier. Adapting arbitrary normal mutation distributions in evolution strategies: the covariance matrix adaptation. In *IEEE Congress on Evolutionary Computation*, pages 312–317, 1996.

[9] C. Igel, N. Hansen, and S. Roth. Covariance matrix adaptation for multiobjective optimization. *Evolutionary Computation*, 15(1):1–28, 2007.

[10] P. Justino and A. Clément. Hydrodynamic performance for small arrays of submerged spheres. In *5th European Wave Energy Conference*, 2003.

[11] O. Krause, T. Glasmachers, N. Hansen, and C. Igel. Unbounded Population MO-CMA-ES for the Bi-Objective BBOB Test Suite. In *Genetic and Evolutionary Computation Conference*, pages 1177–1184. ACM, 2016.

[12] M. Lagoun, A. Benalia, and M. Benbouzid. Ocean wave converters: State of the art and current status. In *IEEE Int. Energy Conf.*, pages 636–641, 2010.

[13] I. López, J. Andreu, S. Ceballos, I. M. de Alegría, and I. Kortabarria. Review of wave energy technologies and the necessary power-equipment. *Renewable and Sustainable Energy Reviews*, 27:413–434, 2013.

[14] P. A. Lynn. *Electricity from Wave and Tide: An Introduction to Marine Energy*. John Wiley & Sons, 2013.

[15] A. McCabe, G. Aggidis, and M. Widden. Optimizing the shape of a surge-and-pitch wave energy collector using a genetic algorithm. *Renewable Energy*, 35(12):2767–2775, 2010.

[16] P. McIver. Arrays of wave-energy devices. In *5th International Workshop on Water Waves and Floating Bodies*, Oxford, UK, 1995.

[17] M. Mohamed, G. Janiga, E. Pap, and D. Thévenin. Multi-objective optimization of the airfoil shape of Wells turbine used for wave energy conversion. *Energy*, 36(1):438–446, 2011.

[18] V. S. Neary, M. Lawson, M. Previsic, A. Copping, K. C. Hallett, A. Labonte, J. Rieks, and D. Murray. Methodology for design and economic analysis of marine energy conversion (MEC) technologies. Technical report, Sandia National Laboratories, 2014.

[19] G. Nunes, D. Valério, P. Beirao, and J. S. Da Costa. Modelling and control of a wave energy converter. *Renewable Energy*, 36(7):1913–1921, 2011.

[20] J. T. Scruggs, S. M. Lattanzio, A. A. Taflanidis, and I. L. Cassidy. Optimal causal control of a wave energy converter in a random sea. *Applied Ocean Research*, 42(2013):1–15, 2013.

[21] N. Y. Sergiienko, B. S. Cazzolato, B. Ding, and M. Arjomandi. Frequency domain model of the three-tether WECs array. `http://tiny.cc/ThreeTether`, 2016. code: `http://tiny.cc/OptEn`, [Online; accessed 1-March-2018].

[22] M. Wagner, J. Day, and F. Neumann. A fast and effective local search algorithm for optimizing the placement of wind turbines. *Renewable Energy*, 51:64–70, 2013.

[23] G. X. Wu. Radiation and diffraction by a submerged sphere advancing in water waves of finite depth. *Mathematical and Physical Sciences*, 448(1932): 29–54, 1995.

[24] J. Wu, S. Shekh, N. Y. Sergiienko, B. S. Cazzolato, B. Ding, F. Neumann, and M. Wagner. Fast and effective optimisation of arrays of submerged wave energy converters. In *GECCO*, pages 1045–1052. ACM, 2016.